Clin. Lab. 2024;70:XXX-XXX


## ORIGINAL ARTICLE

# Hsa_Circ_0002762 may be a New Marker for the Gastric Cancer Diagnosis and Prognosis

Jierong Wang [1, 2, 4], Chunyan Mao [1, 2], Ronghua Fang [1, 2], Wentao Yuan [1, 2], Kun Wang [4], Hui Cong [1, 3]

[1] *Department of Laboratory Medicine, Affiliated Hospital of Nantong University, Nantong, Jiangsu, China*
[2] *Medical School of Nantong University, Nantong University, Nantong, Jiangsu, China*
[3] *Department of Blood Transfusion, Affiliated Hospital of Nantong University, Nantong, Jiangsu, China*
[4] *Department of Laboratory Medicine, Dafeng People's Hospital, Yancheng, Jiangsu, China*

### SUMMARY

***Background:*** **The global incidence and mortality rate of gastric carcinoma (GC) persists at elevated levels, often manifesting no overt symptoms in its early stages. Hsa_circ_0002762 has been identified as an important modulator in cervical cancer. This study aims to explore its role in the context of GC.**
***Methods:*** **A quantitative real-time polymerase chain reaction (qPCR) was implemented to assess the expression level of hsa_circ_0002762. The over-expression was confirmed through an examination of 28 cases of gastric cancer and their corresponding adjacent tissues. In addition, plasma samples from 78 healthy individuals, from 45 benign gastritis patients, and from 106 gastric cancer patients were collected, and the diagnostic efficacy was assessed by analyzing the receiver operating characteristic (ROC) curve. Simultaneously, postoperative specimens from 36 GC cases were collected, and a Kaplan-Meier survival analysis curve was used to evaluate the prognosis of GC.**
***Results:*** **The study revealed an up-regulation in the expression of hsa_circ_0002762 in gastric cancer plasma and tissues. The area under the receiver operating characteristic (ROC) curve for serum hsa_circ_0002762 was 0.784 (95% CI: 0.719 - 0.851), indicating a higher diagnostic efficiency compared to CEA (0.687, 95% CI: 0.611 - 0.763) and CA199 (0.699, 95% CI: 0.625 - 0.744). Combining these three biomarkers demonstrated an increased sensitivity in the diagnostic effectiveness. Finally, postoperative dynamic monitoring revealed a practical utility in predicting the clinical prognosis using serum has_circ_0002762.**
***Conclusions:*** **The findings from our study suggest that hsa_circ_0002762 holds promise as a novel diagnostic and prognostic marker for individuals with GC.**
**(Clin. Lab. 2024;70:xx-xx. DOI: 10.7754/Clin.Lab.2024.231212)**

**Correspondence:**
Hui Cong
Department of Laboratory Medicine
Affiliated Hospital of Nantong University
Xisi Rd, No. 20, Nantong 226001
Jiangsu
China
Email: huicjs@163.com

Kun Wang
Department of Laboratory Medicine
Dafeng People's Hospital
Xingfu East Rd, No. 139, Yancheng 224100
Jiangsu
China
Email: dfwangkun@163.com

### KEYWORDS

Hsa_circ_0002762, diagnosis, prognosis, gastric cancer

Manuscript accepted January 1, 2024

## INTRODUCTION

Gastric carcinoma (GC) comprises a diverse group of diseases characterized by a high morbidity and mortality 1, a low survival rate, and a poor prognosis 2, making it a significant contributor to cancer-related deaths globally. Through extensive molecular studies, a distinctive pathogenesis and an active carcinogenic pathway specific to GC have been identified 3. The incidence of GC is notably higher in men, with data from Cancer Incidence in Five Continents indicating a standardized incidence ratio of 4.0:1 for gastric cardia cancer (GCC) and 2.1:1 for gastric non-cardia cancer (GNC) in males compared to females 4. Given its aggressive nature and susceptibility to distant metastasis, GC often leads to poor treatment outcomes and survival rates 5. Distant metastasis, in particular, results in a dismal five-year survival rate as low as 6% 6. The initial stages of GC are characterized by occult symptoms, lacking typical manifestations. This often leads to misinterpretation of symptoms as common gastrointestinal issues, causing a delay in optimal treatment 7. The current gold standard for diagnosing gastric cancer involves pathological examinations following an invasive endoscopic biopsy 8. This procedure is not only painful but poses challenges topatients' acceptance. In contrast, blood biomarkers offer a non-invasive and objective alternative to endoscopy 9. Commonly used GC biomarkers include osteopontin (OPN), Helicobacter pylori antibody (Hp-Ab), PGI/II, gastric cancer-associated antigen (MG7-Ag), CA 72-4, tissue polypeptide-specific antigen (TPS), CA 19-9, and CEA among others 1012. However, their clinical utility is hampered by a low sensitivity and accuracy. For instance, the combined detection of PGI/II-HpAb-OPN exhibits a sensitivity of only 70.2%, and the prediction probability is 0.493 13. Therefore, the quest for new biomarkers remains crucial in enhancing diagnostic precision and in improving clinical outcomes for patients with GC.

Circular RNA (circRNA) stands out as a unique single-stranded RNA generated through the reverse cleavage of precursor mRNA 14. The circRNA structure is defined by a covalently closed configuration, devoid of 5' - 3' polarity and a poly(A) tail, rendering it structurally stable and resistant to degradation by exonucleases. CircRNA exerts its regulatory influence on genetic expression at the transcriptional level by acting as a sponge for miRNA, by encoding proteins or short peptides with biological activity, and by binding proteins post-transcription to disrupt normal genetic function 15. The aberrant expression of circRNA plays a pivotal role in the progression of various tumors through mechanisms like transcriptional repression and post-transcriptional regulation 16. The molecular diagnosis of tumors has become a focal point of extensive and comprehensive research, marked by significant clinical trials. This research provides valuable insights guiding the diagnostic, therapeutic, and prognostic aspects of disease management 17. Hsa_circ_0002762 has been recognized as a key modulator in cervical cancer, but its significance in other tumor types remains unclear. This study is designed to explore its role in GC.

## MATERIALS AND METHODS

### Sample collection

Participants in this study comprised patients and healthy individuals at the Affiliated Hospital of Nantong University (Nantong, China). Plasma specimens were systematically collected, including 106 specimens from patients with newly diagnosed gastric cancer (excluding other cancer patients), 45 from patients with benign gastritis, and 76 from subjects undergoing healthy medical examinations. Additionally, a total of 28 pairs of tissues, consisting of GC samples and their corresponding paracancer tissues, were meticulously collected. Simultaneously, 36 postoperative serum samples from GC patients were obtained to validate the prognostic implications of the findings. All collected specimens were diligently stored in a freezer at -80°C until the commencement of subsequent experiments. The procedural framework for this work received approval from the Ethics Committee of the Affiliated Hospital of Nantong University.

### Cells culture

Gastric cancer cells (HGC-27, SGC-7901, MKN-45, MGC-803) and GES-1 were procured from the Stem Cell Bank of the Chinese Academy of Sciences (Shanghai, China), with GES-1 serving as the reference cell line. The complete culture medium comprised 10% fetal bovine serum (FBS, Gibco), 1% double antibiotics (penicillin and streptomycin), and RPMI-1640 medium (Corning). Cells were cultured in the complete medium, thoroughly mixed, and incubated in a humidified incubator with 5% carbon dioxide to create optimal growth conditions.

### Total RNA extraction and reverse transcription (RT)

Total RNA extraction from GC tissues and cells followed the guidelines provided by the TRIzol reagent (Shanghai, Co., Ltd., China). Total RNA extraction was performed for GC serum using TRIzol LS reagent (BioTeke Corporation, China). The concentration and purity of the extracted RNA were subsequently assessed using a spectrophotometer (Thermo Fisher Scientific, USA). Following the manufacturer's instructions for the reverse transcription kit (Biosharp, China), the obtained total RNA underwent reverse transcription, transforming it into single-stranded cDNA. This cDNA served as the foundation for subsequent PCR experiments.

### Real-Time quantitative PCR (qRT-PCR)

The qRT-PCR analysis was conducted utilizing the LightCycler ® 480 (Roche, Switzerland) amplification apparatus. Gene sequences targeted included: hsa_-

circ_0002762 (Forward: 5´-GTCTCAAACTCC TGGG CTCAAGTG-3´; Reverse: 5´-GGCTAGGCAT GGTG GCTCATTG-3´); 18S rRNA (Forward: 5´-GTAACCC GTT GAACCCCATT-3´; Reverse: 5´-CCATCCAATC GGTAGTAGCG-3´). The reference gene 18S rRNA was used to standardize the expression quantification across all specimens. The levels of hsa_circ_0002762 were determined using the $2^{-\Delta\Delta CT}$ method for relative quantitative calculation.

**Nucleoplasm separation assay**

The Nucleoplasmic Extraction Kit (Beyotime, China) was used, following the provided procedures, to segregate nuclear and cytoplasmic RNA from SGC-7901 and MGC-803 cells. Cells were washed with PBS, harvested by using a cell scraper, and subjected to ice treatment. Subsequently, cell extraction reagent A was added, and cells were vigorously vortexed, followed by an incubition period on ice for 10 - 15 minutes. Cell extraction reagent B was introduced, and the mixture was centrifuged at 15,000 g for 5 minutes, resulting in the separation of the nucleus at the bottom sediment and the cytoplasm in the supernatant. The collected supernatant, containing cytoplasmic RNA, was transferred to clean EP tubes for further experiments. The nucleus-containing particles were then combined with a nucleoprotein extraction reagent. After vortexing and ensuring uniformity through incubation on ice, the mixture underwent centrifugation at 15,000 g for 10 minutes. The resulting supernatant, now nucleoprotein, was carefully transferred to a new EP tube for subsequent RNA extraction. Finally, cytoplasmic and nuclear RNA solutions were obtained and stored in a refrigerator at -80°C for further analysis.

**Statistical analysis**

Statistical analysis was performed, using the SPSS 27.0 software (IBM Corporation, Armonk, NY, USA), for the evaluation of clinicopathological parameters, while GraphPad Prism 9.5 was used for chart production and data analysis. Univariate analysis of variance, logistic regression analysis, and the chi-squared test were used for statistics analysis. The ROC curve method was applied to evaluate the clinical diagnostic efficacy of hsa_circ_0002762, CEA, and CA19-9. Statistical significance was determined at $p < 0.05$, indicating the threshold for statistical significance in the analyses.

## RESULTS

**Evaluation of the methodological performance of hsa_circ_0002762**

The qRT-PCR analysis revealed a significant up-regulation in the expression of hsa_circ_0002762 in GC tissues ($p = 0.0034$), as illustrated in Figure 1A. To assess the concentration gradient, cDNA was diluted at ratios of 1:10, 1:100, 1:1,000, 1:10,000, 1:100,000. The qRT-PCR analysis of hsa_circ_0002762 and 18S rRNA Ct values in the gradient samples yielded a linear equation for hsa_circ_0002762 ($Y = –1.961X + 27.34$) with an R2 value of 0.9958 (Figure 1B). Similarly, the linear equation for 18S rRNA was determined as $Y = –2.786X + 6.130$ with an R2 value of 0.9930 (Figure 1C). The high linear correlation indicates the feasibility of the experiment. Furthermore, cDNA samples from GC cells (SGC-7901) were selected according to the precision evaluation document criteria of the EP5-A2 quantitative test method. One sample was tested daily and repeated four times per sample for five consecutive days. The results demonstrated excellent intra-and inter-batch precision for hsa_circ_0002762 and 18S rRNA, with CV values below 5% (Table 1).

**Validation of the stability of hsa_circ_0002762**

To ascertain the stability of hsa_circ_0002762 in liquid biopsy, we evenly mixed 20 serum samples and divided the mixed serum into two groups. The first group was subdivided into six parts, each incubated at room temperature for 0, 2, 4, 8, 15 and 24 hours, respectively. Subsequent detection of the corresponding Ct values for hsa_circ_0002762 and 18S rRNA, with no statistical difference ($p > 0.05$), as depicted in Figure 2A. The second group, divided into five parts, underwent repeated freezing and thawing for 0, 3, 5, 8, and 10 cycles, respectively. The corresponding changes in the Ct values were tested, and the results indicated no significant changes in the Ct values of hsa_circ_0002762 and 18S rRNA, with no statistical difference ($p > 0.05$) as illustrated in Figure 2B. The dissolution curves of hsa_circ_0002762 and 18S rRNA demonstrated a unimodal pattern through RT-qPCR analysis (Figure 2C).

**Relation between hsa_circ_0002762 expression and clinicopathological parameters in GC patients**

The 106 GC patients were categorized based on various clinically relevant indicators. The expression level of hsa_circ_0002762 was stratified into low and high expression groups using the median, and the correlation between hsa_circ_0002762 levels and clinicopathological parameters was examined. Statistical analysis revealed a significant correlation between the plasma hsa_circ_0002762 levels in GC patients and the tissue differentiation grade, TNM stage, nerve/vascular invasion, and lymphatic metastasis (*** $p < 0.001$). However, no significant correlation was observed with clinicopathological parameters such as Lauren stage, gender, age, and tumor size ($p > 0.05$) (Table 2).

**Diagnostic efficacy of hsa_circ_0002762**

The plasma level of circ_0002762 in GC patients was assessed using qRT-PCR. The relative expression level of plasma hsa_circ_0002762 in GC patients was significantly higher than in gastritis patients and in the negative control group (*** $p < 0.0001$). However, no substantial variation was observed between the plasma levels of gastritis patients and the negative control group ($p = 0.9467$) (Figure 3A). ROC curves were constructed

**Table 1. The intra-lot and inter-lot precision of hsa_circ_0002762 and 18S.**

| | | Hsa_circ_0002762 | 18S |
|---|---|---|---|
| Intra-lot | Mean ± SD | 25.457 ± 0.266 | 8.509 ± 0.258 |
| | CV (%) | 1.04 | 3.03 |
| Inter-lot | Mean ± SD | 25.580 ± 0.316 | 8.482 ± 0.309 |
| | CV (%) | 1.24 | 3.64 |

**CV - Coefficient of Variance.**

**Table 2. Relation of hsa_circ_0002762 levels to clinic pathological parameters in gastric cancer patients.**

| Parameter | n | Hsa_circ_0002762 high (n = 53) | Hsa_circ_0002762 low (n = 53) | $\chi 2$ value | p-value |
|---|---|---|---|---|---|
| Gender | | | | 4.566 | 0.052 |
| Male | 53 | 32 | 21 | | |
| Female | 53 | 21 | 32 | | |
| Age (years) | | | | 0.340 | 0.698 |
| ≤ 68 | 51 | 27 | 24 | | |
| > 68 | 55 | 26 | 29 | | |
| Tumor size (cm) | | | | 3.169 | 0.113 |
| ≤ 4cm | 63 | 36 | 27 | | |
| > 4cm | 43 | 17 | 26 | | |
| Histological differentiation | | | | 57.396 | < 0.001 *** |
| Well-Moderate | 53 | 7 | 46 | | |
| Poor | 53 | 46 | 7 | | |
| Lymphatic metastasis | | | | 30.260 | < 0.001 *** |
| Yes | 74 | 24 | 50 | | |
| No | 32 | 29 | 3 | | |
| Nerve/vascular invasion | | | | 26.658 | < 0.001 *** |
| Yes | 64 | 19 | 45 | | |
| No | 42 | 34 | 8 | | |
| TNM stage | | | | 41.153 | < 0.001 *** |
| I and II | 51 | 42 | 9 | | |
| III and IV | 55 | 11 | 44 | | |
| Lauren classification | | | | 2.779 | 0.249 |
| Intestinal | 37 | 17 | 20 | | |
| Diffuse | 36 | 22 | 14 | | |
| Mixed | 33 | 14 | 19 | | |

**Statistical analysis was performed by using the chi-squared test. * p < 0.05 was considered significant.**

based on the plasma levels of circ_0002762 in 106 GC patients and 78 normal controls to evaluate the diagnostic efficacy of hsa_circ_0002762. The AUC value of plasma hsa_circ_0002762 was 0.784 (95% CI: 0.719 – 0.851) (Figure 3B), demonstrating superior diagnostic efficacy compared to CEA (0.687, 95% CI: 0.611 - 0.763) (Figure 3C) and CA19–9 (0.699, 95% CI: 0.625 - 0.744) (Figure 3D). The AUC value of hsa_circ_0002762 combined with CEA was 0.812 (95% CI: 0.752 - 0.873) (Figure 3E), and when combined with

**Table 3. Evaluation of the clinical diagnosis values of combination of hsa_circ_0002762, CEA and CA199 in gastric cancer patients and healthy subjects.**

| | SEN (%) | SPE (%) | ACCU (%) | PPV (%) | NPV (%) | AUC (95% CI) |
|---|---|---|---|---|---|---|
| Hsa_circ_0002762 | 90.6 (96/106) | 53.8 (42/78) | 75.0 (138/184) | 67.6 (96/142) | 80.8 (42/52) | 0.784 (0.719 - 0.851) |
| CEA | 40.1 (36/106) | 87.2 (68/78) | 56.5 (104/184) | 31.1 (36/116) | 49.3 (68/138) | 0.687 (0.611 - 0.763) |
| CA19-9 | 46.2 (49/106) | 80.8 (63/78) | 60.9 (112/184) | 40.5 (49/121) | 52.5 (63/120) | 0.699 (0.625 - 0.744) |
| Hsa_circ_0002762+CEA | 93.4 (99/106) | 48.7 (38/78) | 74.5 (137/184) | 67.8 (99/146) | 84.4 (38/45) | 0.812 (0.752 - 0.873) |
| Hsa_circ_0002762+CA19-9 | 95.3 (101/106) | 43.6 (34/78) | 73.4 (135/184) | 67.3 (101/150) | 87.2 (34/39) | 0.828 (0.772 - 0.885) |
| Hsa_circ_0002762+CEA+CA19-9 | 98.1 (104/106) | 38.5 (30/78) | 72.8 (134/184) | 67.5 (104/154) | 93.8 (30/32) | 0.843 (0.789 - 0.897) |

**SEN - sensitivity, SPE - specificity, ACCU - overall accuracy, PPV - positive predictive value, NPV - negative predictive value, AUC - area under the curve, CI - confidence interval.**

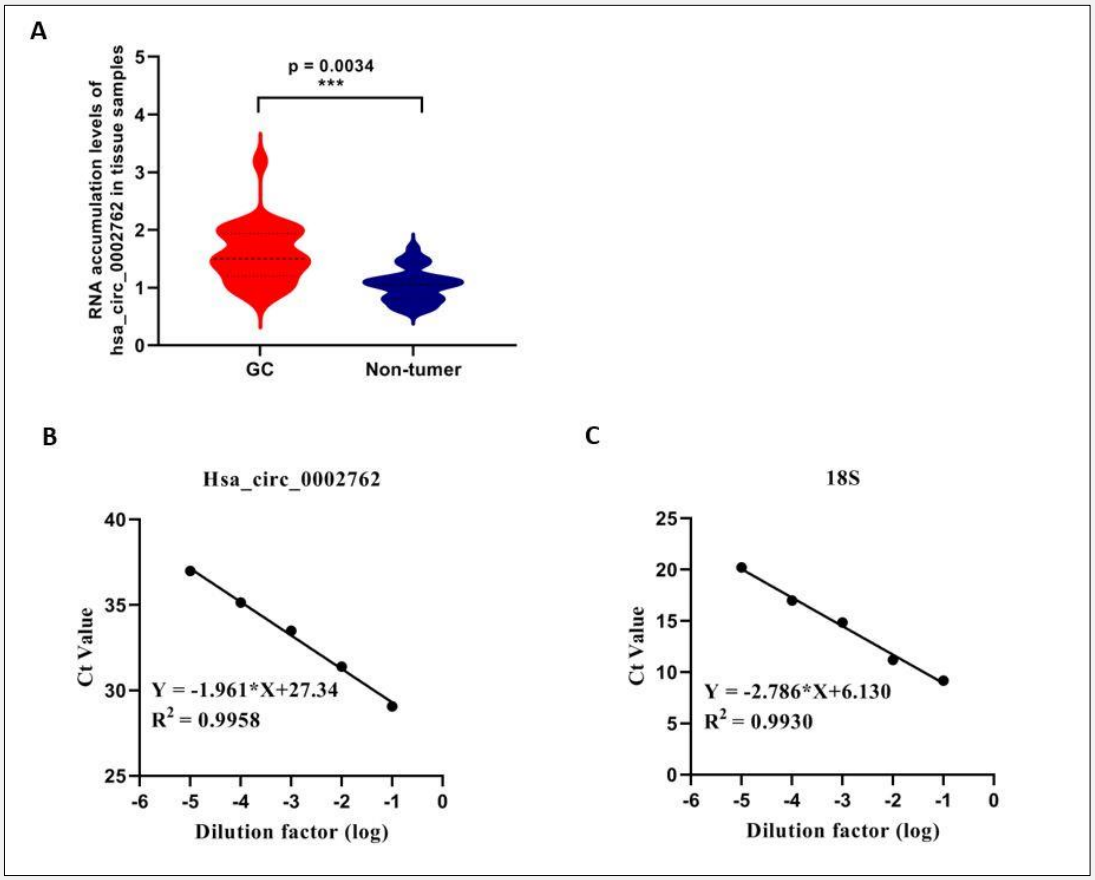


**Figure 1. Evaluation of the methodological performance of hsa_circ_0002762.**

**A - Levels of hsa_circ_0002762 in twenty-eight pairs of GC tissues and the corresponding paracancer tissue samples.**
**B, C - Regression curves of hsa_circ_0002762 and 18S.**

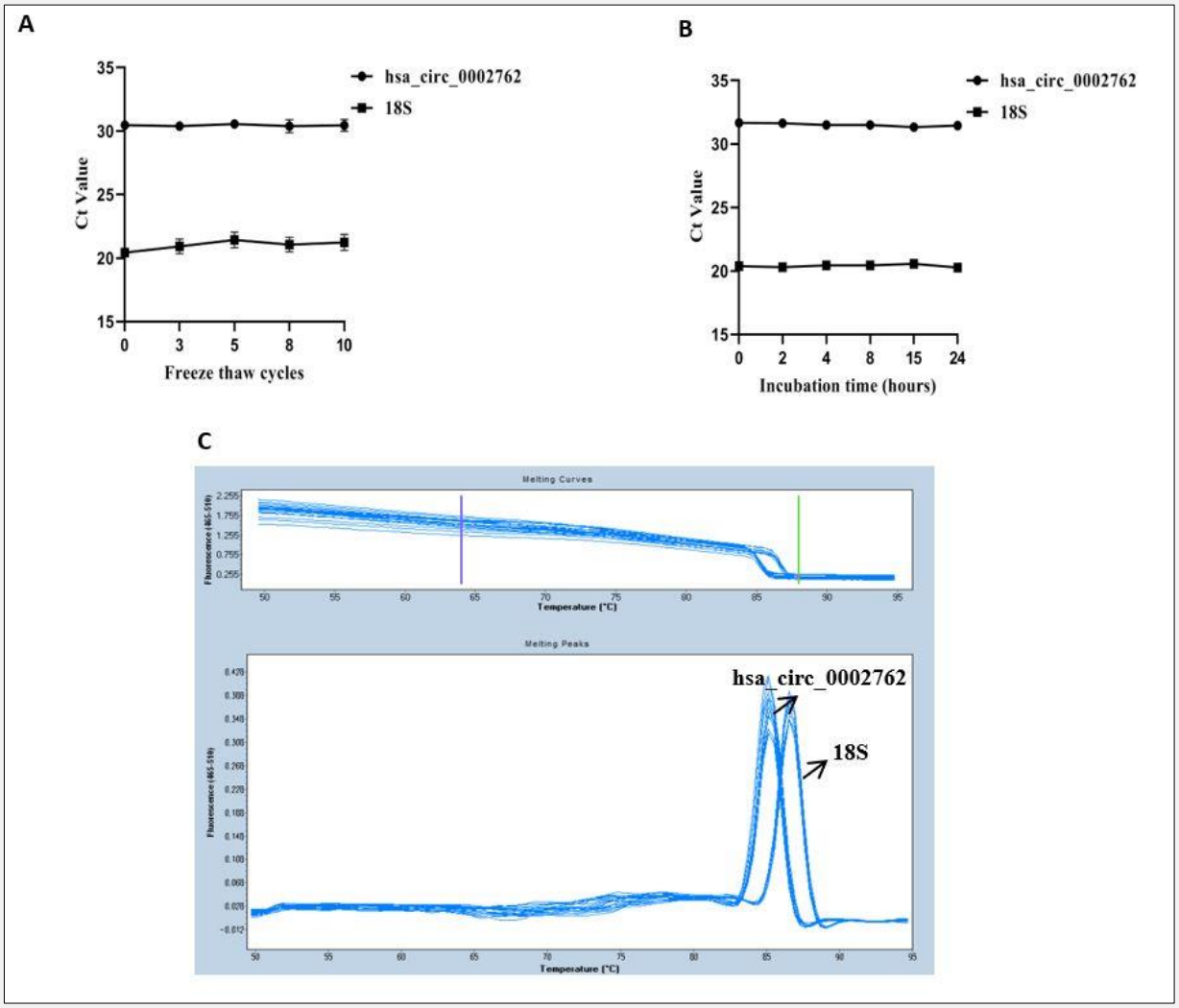


**Figure 2. Verification of the stability of hsa_circ_0002762.**

**A - Stability of serum hsa_circ_0002762 and 18S under multiple freeze-thaw conditions.**
**B - Stability of serum hsa_circ_0002762 and 18S, incubated at room temperature for 0, 2, 4, 8, 15, and 24 hours.**
**C - PCR unimodal curves for hsa_circ_0002762 and 18S.**

CA19-9, it was 0.828 (95% CI: 0.772 - 0.885) (Figure 3F). The combined AUC value of the three markers was 0.843 (95% CI: 0.789 - 0.897) (Figure 3G), indicating that a combined diagnosis enhances the sensitivity of a single marker, reaching up to 98.1% (Table 3). These experiments provide further evidence that supports the potential of hsa_circ_0002762 as a promising biological tumor marker for diagnosing GC.

**Prognostic analysis of hsa_circ_0002762**

To investigate the potential role of hsa_circ_0002762 as a key molecule in GC prognosis, plasma samples were collected from 36 GC patients one week after the operation. The levels of hsa_circ_0002762 were detected by qPCR, revealing a significant decline after the operation (*** $p < 0.001$) (Figure 4A). Kaplan-Meier survival curve analysis indicated a reduced survival rate in the hsa_circ_0002762 (high) group compared to the hsa_circ_0002762 (low) group (Figure 4B). These findings support the notion that hsa_circ_0002762 could serve as a valuable marker for postoperative GC monitoring, with potential clinical applications in prognosis assessment.

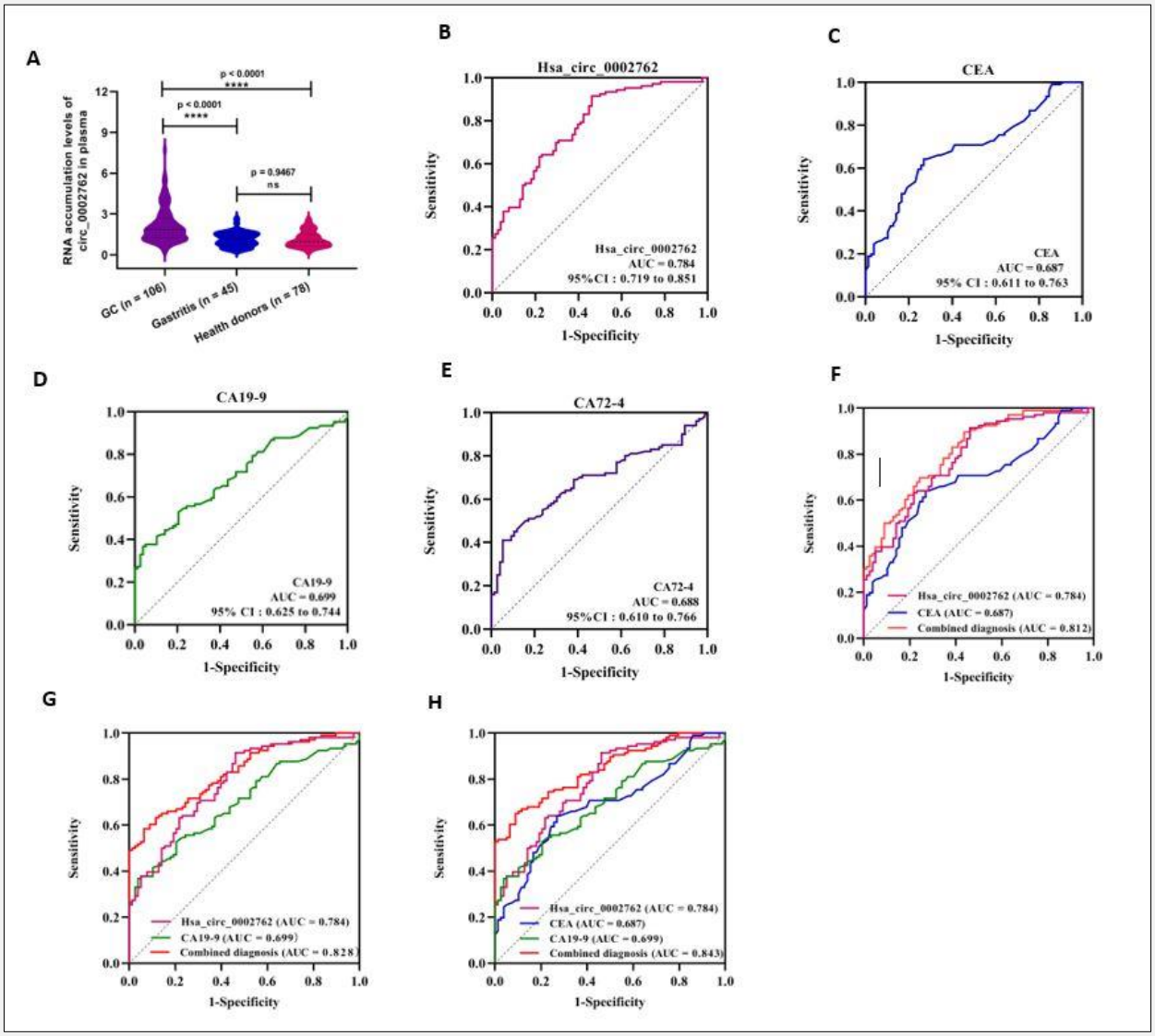


**Figure 3. Expression of plasma hsa_circ_0002762 in GC and evaluation of diagnostic efficacy in GC.**

**A - Levels of plasma hsa_circ_0002762 in GC patients (n = 106), gastritis patients (n = 45) and healthy subjects (n = 78), indicating statistical significance.**
**B - D - ROC curves analysis of plasma hsa_circ_0002762, CEA, and CA19-9 to distinguish between GC patients (n = 106) and healthy subjects (n = 78).**
**E - ROC curves analysis of plasma CA72-4 to distinguish between GC patients (n = 100) and healthy subjects (n = 76).**
**F - H - The combined diagnosis of plasma hsa_circ_0002762, CEA, and CA199 provided better diagnostic results for GC patients (n = 106) and healthy subjects (n = 78).**

### Investigation of the regulatory axis of hsa_ circ_ 0002762 in gastric carcinoma cells

The expression levels of hsa_circ_0002762 in GC cells were assessed through RT-qPCR to elucidate the pathway of hsa_circ_0002762 in gastric carcinoma cells, with GES-1 cells as the control. Notably, hsa_circ_0002762 exhibited significant up-regulation in SGC-7901 and MGC-803 cell lines, while the up-regulation was not statistically significant in MKN-45 and HGC-27 cells (Figure 5A). Additionally, cytoplasmic and nuclear RNA extraction from SGC-7901 and MGC-803 cells, using nuclear-cytoplasmic separation experiments,

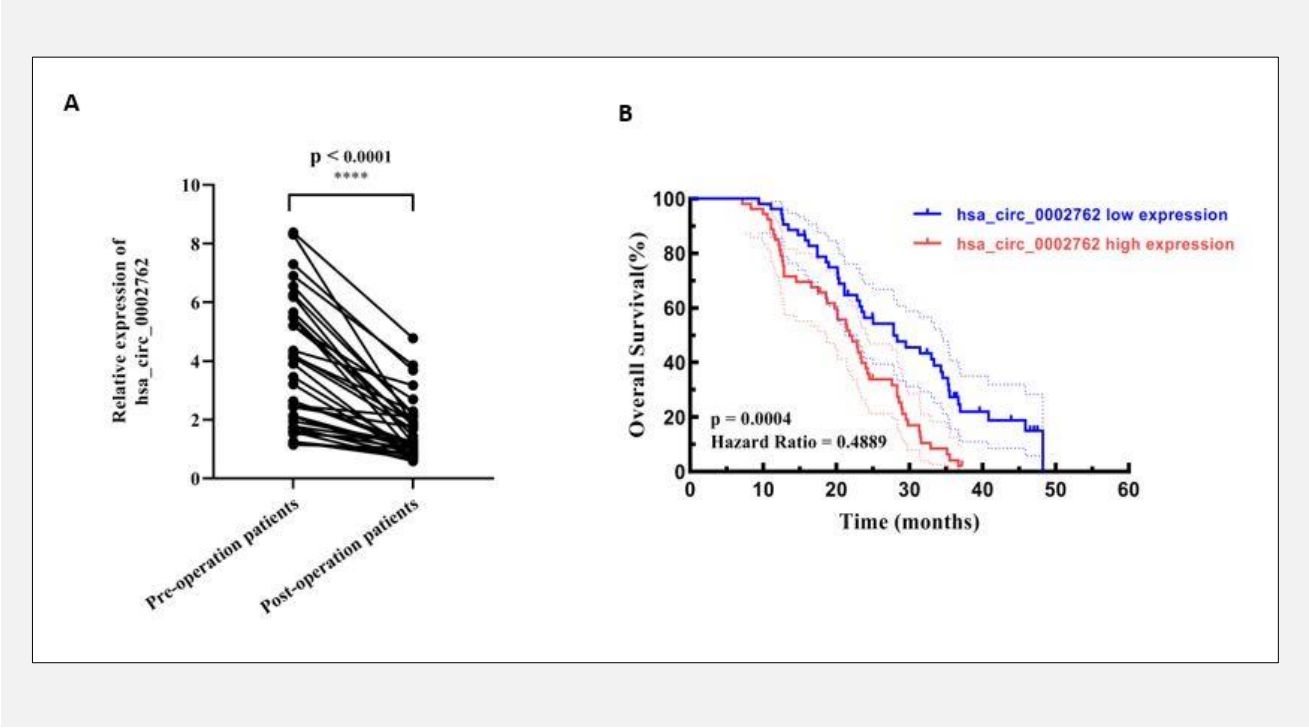


**Figure 4. Prognostic analysis of hsa_circ_0002762.**

**A - Levels of hsa_circ_0002762 in GC patients decreased after surgery (n = 36, p < .0001).**
**B - The survival rate in the hsa_circ_0002762 (high) group was lower than that in the hsa_circ_0002762 (low) group.**

revealed a higher proportion of hsa_circ_0002762 in the cytoplasm, indicating its potential critical role through post-transcriptional regulation (Figure 5B). The circbank and circinteractome databases were utilized to predict target miRNAs binding to hsa_circ_0002762. Differentially expressed miRNAs in GC were obtained from TCGA database analysis using RNA-seq data. The R language analysis identified differentially expressed downstream miRNA that could be modulated by hsa_circ_0002762 ($p < 0.01$, $logFC \geq 1$). PCR validation confirmed the expression of hsa-miR-139-3p, hsa-miR-502-5p, hsa-miR-103a-2-5p, hsa-miR-4677-3p, and hsa-miR-500b-5p. Furthermore, the bioinformatics database (miRDB, TargetScan, miWalk) was used to predict target genes corresponding to the miRNAs, constructing the ceRNA regulatory network centered on hsa_circ_0002762 (Figure 5C). This approach provides a novel avenue for studying the regulatory role of hsa_circ_0002762 in stomach cancer and its impact on GC progression.

## DISCUSSION

Circular RNA (circRNA) represents a subclass of non-coding RNAs (ncRNAs) characterized by a covalently closed circular structure, displaying tissue-specific and species-specific expression patterns. Its unique structural stability and resistance to degradation by RNA exoenzymes have sparked extensive research in the scientific community. The exploration of circRNAs has deepened our understanding of the mechanisms and functions of ncRNAs in eukaryotes. CricDNAs have emerged as a key player in regulatory networks in various diseases. For instance, in age-related macular degeneration (AMD), cricRNA Uxs1 has been identified as a crucial factor promoting choroidal neovascularization (CNV). Through its sponge activity on miR-335-5p, cricRNA Uxs1 stimulates PGF expression and activates the mTOR/p70 S6 k pathway, establishing itself as a therapeutic target for CNV 18. In hepatocellular carcinoma (HCC), circRNAs play diverse roles. Hsa_circ_0051040, up-regulated in HCC tissues, acts as a sponge for miR-569 to regulate ITGAV expression, inducing epithelial-mesenchymal transition (EMT) progression and promoting the occurrence and progression of HCC 19. CircFOXK2, aberrantly expressed in HCC tissues, modulates the miR-484/Fis1 pathway, leading to mitochondrial fission and activating the Warburg effect, ultimately promoting HCC progression 20. Another circRNA, CircTGFBR2, functions as a tumor promoter in hepatocyte exosomes, promoting HCC progression by enhancing ATG5-mediated protective autophagy through the circTGFBR2/miR-205–5p/ATG 5

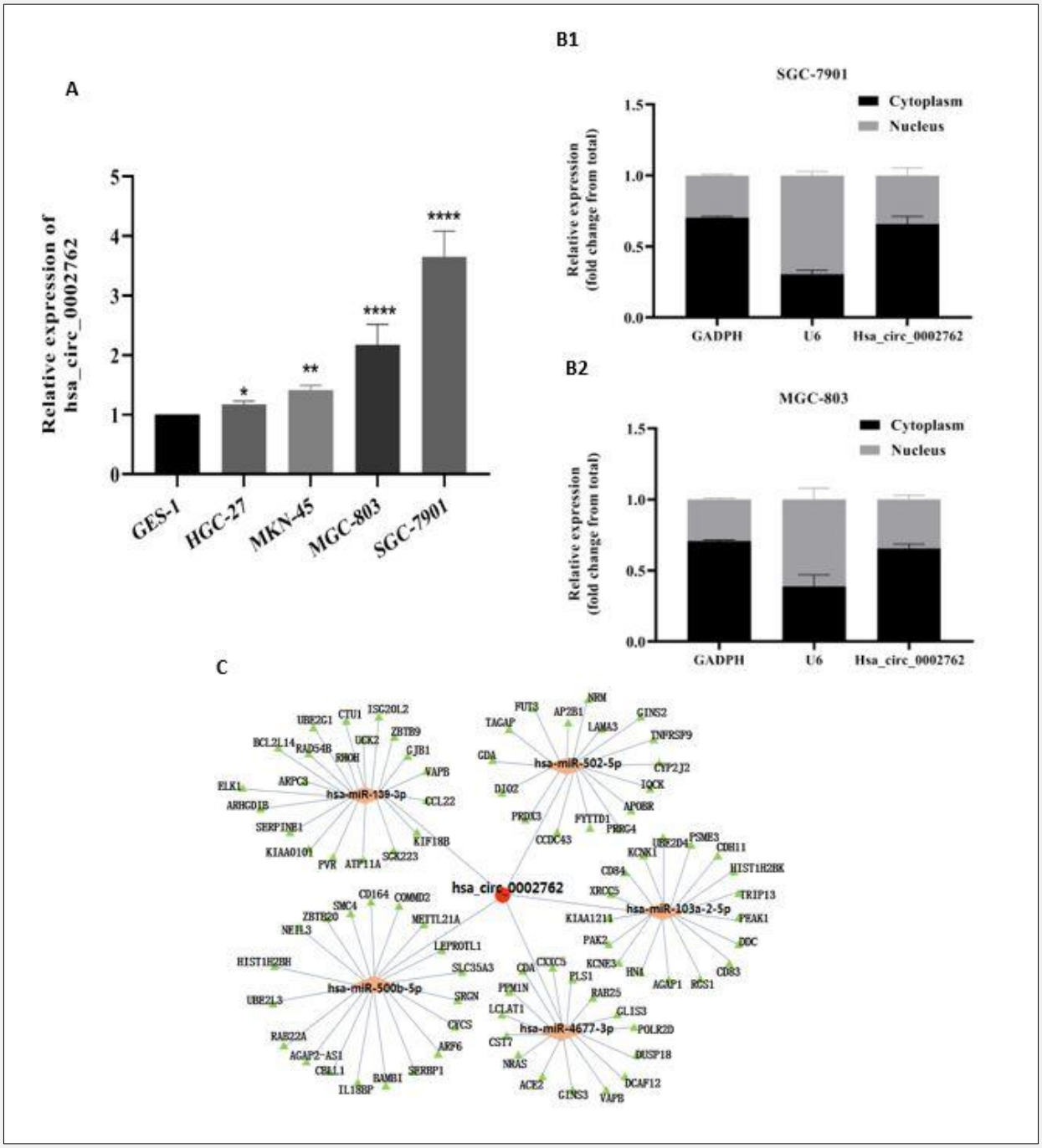


**Figure 5. Investigation of the downstream regulatory network of hsa_circ_0002762 in GC cells.**

**A - Levels of hsa_circ_0002762 in four GC cells.**
**B - The hsa_circ_0002762 was primarily localized in the cytoplasm in the SGC-7901 and MGC-803 cell lines.**
**C - Prediction of hsa_circ_0002762-miRNA-mRNA network map. The red circle represented hsa_circ_0002762, the orange diamond represented five miRNA that could interact with hsa_circ_0002762, while the green triangle represented the target mRNA of the corresponding miRNA, indicating statistical significance (** $p < 0.01$).**

axis 21. Across multiple diseases, circRNAs play a crucial biological role by constructing competitive endogenous RNA networks through sponge-mediated miRNA interactions 22. The expanding knowledge in this field opens avenues for exploring novel therapeutic targets and diagnostic markers in various pathological conditions.

Numerous studies have underscored the pivotal role of circRNA in GC, acting as both oncogenic drivers and tumor suppressors. These circRNAs exert their regulatory influence in diverse mechanisms, contributing significantly to the development and prognosis of GC. Circ IPO7 exhibits down-regulation in GC tissues and cells, and its mechanism involves dissociating caprin-1 from ribosomes, thereby inhibiting the translation of EGFR and mTOR. This inhibition culminates in the suppression of gastric cancer cell proliferation, presenting circ_IPO7 as a potential tumor suppressor in GC 23. Has_circ_0052001 is up-regulated in GC tissues and promotes GC development. It achieves this by activating the MAPK signaling pathway through sponge-mediated regulation of miR-608. The insights gained from studying has_circ_0052001 offer novel therapeutic ideas for treating GC patients 24. CircMAP2K2, another circRNA, regulates the PCBP 1/GPX 1 axis via proteasome mediation. This regulation activates the AKT/GSK3β/EMT signaling pathway, contributing to GC cell proliferation and metastasis. A novel therapeutic strategy involves utilizing the epigallocatechin-3-gallate-lysozyme fibrils delivery system carrying si-circMAP2K2, providing a promising tool for GC treatment 25. CircMTHFD2L, encoding the protein CM-248aa, competitively targets the acidic domain of the SET nuclear oncogene (SET). This unique mechanism leads to the inhibition of gastric cancer progression, presenting CircMTHFD2L as a promising therapeutic target in GC 26. It is crucial to emphasize that the aberrant expression of circRNAs plays a critical role in the etiology of oncology, underscoring the complexity and significance of cricRNA-mediated regulation in GC.

This study successfully validated the distinctive expression pattern of hsa_circ_0002762 in the GC plasma and tissues, suggesting its potential as a latent marker that could enhance GC's diagnostic and prognostic capabilities. Recent research has highlighted the up-regulation of hsa_circ_0002762 in cervical cancer (CC), where it competitively regulates ASF1B expression through miR-122-5p, thereby contributing to CC progression 27. While hsa_circ_0002762 is recognized as a key regulator in CC, its expression in other malignancies remains unclear. To begin with, our assays demonstrated the unimodal specificity of hsa_circ_0002762 in GC plasma, tissues, and cells, using 18S as the internal reference. Statistical analysis showed that both hsa_circ_0002762 and 18S rRNA, detected by RT-qPCR, exhibited a robust linear correlation, affirming the method's feasibility. Furthermore, adhering to the accuracy evaluation standards outlined in the EP5-A2 quantitative detection method, the RT-qPCR detected hsa_circ_0002762, and 18S demonstrated excellent intra-lot and inter-lot precision, with a coefficient of variation consistently below 4%. These findings underscore the accuracy and reliability of the employed methodology.

In our investigation, we meticulously assessed the expression levels of hsa_circ_0002762 in both GC tissues and plasma using RT-qPCR. The findings revealed a significant up-regulation of hsa_circ_0002762 in GC patients compared to adjacent tissues. Similarly, plasma levels in GC patients were notably higher than those in healthy subjects and gastritis patients. An exploration of the correlation between plasma hsa_circ_0002762 levels and clinicopathological parameters indicated a substantial association with histological differentiation degree, lymph node metastasis, nerve/vascular differentiation degree, and TNM stage. This suggests that hsa_circ_0002762 may be intricately linked to GC growth, progression, and malignancy. Further delving into its diagnostic efficacy, we found that the AUC of hsa_circ_0002762 surpassed conventional gastric cancer diagnostic markers such as CA19-9 and CEA. Both one-way variance and logistic regression analyses demonstrated superior diagnostic efficiency for hsa_circ_0002762. Notably, combining the three biomarkers significantly elevated the sensitivity of gastric cancer diagnosis. Additionally, postoperative GC patients exhibited significantly lower plasma expression levels, and Kaplan-Meier survival curve analysis indicated the prognostic potential of hsa_circ_0002762 in dynamic monitoring. Examining its role in GC cells, RT-qPCR results showed a significant up-regulation of hsa_circ_0002762 in SGC-7901 and MGC-803 cells, suggesting its potential as an oncogene in GC. Nuclear-plasmic separation experiments confirmed its predominant location in the cytoplasm. Further investigation of the ceRNA network revealed hsa_circ_0002762's ability to target and bind miR-139-3p, miR-502-5p, miR-103a-2-5p, miR-4677-3p, and miR-500b-5p. These miRNAs exhibited an abnormal expression in GC tissues and are associated with various biological regulatory mechanisms in GC progression. For instance, circ-PTPDC1 and circPTK2, targeted by miR-139-3p, have been implicated in regulating ELK1 and promoting GC progression 2829. CircDLST, targeted by 502–5p, plays a role in GC metastasis by activating NRAS/MEK1/ERK1/2 signaling 30. Hsa_circ_0000144, influenced by miR-502-5p, is involved in oxaliplatin resistance in GC cells 31. The experiment demonstrated that miR-502-5p down-regulated the expression of PD-L1 at transcriptional and post-transcriptional levels to inhibit the progression of gastric cancer 32. MiR-103a-2-5p, with a binding site at the 3´-UTR of SMYD3, inhibited its translation, while SMYD3 directly bound to the promoter region of TWIST3, enhancing its transcription. LTSCCAT, targeting miR-103a-2-5p, regulated the SMYD3/TWIST1 axis and promoted tongue squamous cell carcinoma metastasis 33. CircZDBF2 was found to advance OSCC progression by elevating RNF145 (ring finger protein

145) levels through miR-362-5p and miR-500b-5p, thereby activating the NFκB signaling pathway 34. MiR-4677-3p, observed to be down-regulated in GC tissues and cells, is implicated in the proliferation and metastasis of GC cells through the CEMIP-PI3K/AKT signaling pathway 35.This intricate ceRNA network, centered on hsa_circ_0002762 and targeting five miRNAs, showcases its diverse roles in gastric cancer progression.

## CONCLUSION

In conclusion, our study highlights the significant upregulation of hsa_circ_0002762 in the plasma of GC patients. Combining its detection with serum CEA and CA19–9 enhances the sensitivity of gastric cancer detection, potentially reducing misdiagnosis rates. Hsa_circ_0002762 emerges as a promising auxiliary diagnostic marker and a potential diagnostic indicator for GC. Our association analysis underscores the close correlation between hsa_circ_0002762 and GC tissue differentiation degree and lymph node metastasis, suggesting a potential role in regulating GC metastasis. However, further *in vitro* and *in vivo* studies are essential to validate these conclusions. This study's limited collection scope and relatively small sample size call for additional investigation focusing on gathering more cases and exploring the prognostic survival time of gastric cancer patients. The specific mechanism of hsa_circ_0002762 warrants further validation, and the bioinformatics predicted hsa_circ_0002762-miRNA-mRNA regulatory network requires thorough demonstration. Deepening our understanding of the role of hsa_circ_0002762 in gastric carcinoma advancement will pave the way for uncovering its latent functions in GC treatment and prognosis. Ongoing research efforts will contribute to unveiling the intricate molecular landscape and clinical implications of hsa_circ_0002762 in GC.

**Source of Funds:**
This work was supported by key medical research projects of the Jiangsu Provincial Health Commission (ZD 2022008); Jiangsu Provincial Key Medical Discipline (Laboratory) ZDXK202240.

**Data Availability Statement:**
The data that support the findings of this study are available from the corresponding authors upon reasonable request.

**Declaration of Interest:**
The authors report no competing financial interests.

**References:**

1. Thrift AP, Wenker TN, El-Serag HB. Global burden of gastric cancer: epidemiological trends, risk factors, screening and prevention. Nat Rev Clin Oncol 2023;20(5):338-49. (PMID: 36959359)
2. Chen D, Fu M, Chi L, et al. Prognostic and predictive value of a pathomics signature in gastric cancer. Nat Commun 2022;13(1): 6903. (PMID: 36371443)
3. Alsina M, Arrazubi V, Diez M, Tabernero J. Current developments in gastric cancer: from molecular profiling to treatment strategy. Nat Rev Gastroenterol Hepatol 2023;20(3):155-70. (PMID: 36344677)
4. Wang S, Zheng R, Arnold M, et al. Global and national trends in the age-specific sex ratio of esophageal cancer and gastric cancer by subtype. Int J Cancer 2022;151(9):1447-61. (PMID: 35678331)
5. Degu A, Karimi PN, Opanga SA, Nyamu DG. Predictors of survival outcomes among patients with gastric cancer in a leading tertiary, teaching and referral hospital in Kenya. Cancer Med 2023;12(4):4147-60. (PMID: 36172986)
6. Kakeji Y, Ishikawa T, Suzuki S, et al.; Registration Committee of the Japanese Gastric Cancer Association. A retrospective 5-year survival analysis of surgically resected gastric cancer cases from the Japanese Gastric Cancer Association nationwide registry (2001-2013). Gastric Cancer 2022;25(6):1082-93. (PMID: 35790645)
7. Wang Z, Wang Q, Chen C, et al. NNMT enriches for AQP5+ cancer stem cells to drive malignant progression in early gastric cardia adenocarcinoma. Gut 2023;73(1):63-77. (PMID: 36977555)
8. Suzuki H, Ono H, Hirasawa T, et al.; J-WEB/EGC group. Long-term Survival After Endoscopic Resection For Gastric Cancer: Real-world Evidence From a Multicenter Prospective Cohort. Clin Gastroenterol Hepatol 2023;21(2):307-18.e2. (PMID: 35948182)
9. Ma S, Zhou M, Xu Y, et al. Clinical application and detection techniques of liquid biopsy in gastric cancer. Mol Cancer 2023; 22(1):7. (PMID: 36627698)
10. Deng D, Zhang Y, Zhang R, et al. Circulating Proteins and Metabolite Biomarkers in Gastric Cancer: A Systematic Review and Meta-analysis. Arch Med Res 2023;54(2):124-34. (PMID: 36759293)
11. Nagasaki N, Ito M, Boda T, et al. Identification of Helicobacter pylori-related gastric cancer risk using serological gastritis markers and endoscopic findings: a large-scale retrospective cohort study. BMC Gastroenterol 2022;22(1):299. (PMID: 35725370)
12. Wu S, Qu X, Wang N, et al. MG7-Ag, hTERT, and TFF2 identified high-risk intestinal metaplasia and constituted a prediction model for gastric cancer. Chin Med J (Engl) 2023;136(5):610-2. (PMID: 36914955)
13. Sun L, Tu H, Chen T, et al. Three-dimensional combined biomarkers assay could improve diagnostic accuracy for gastric cancer. Sci Rep 2017;7(1):11621. (PMID: 28912586)
14. Zhang L, Lu C, Zeng M, Li Y, Wang J. CRMSS: predicting circRNA-RBP binding sites based on multi-scale characterizing sequence and structure features. Brief Bioinform 2023;24(1) bbac530. (PMID: 36511222)

15. Chen R, Wang SK, Belk JA, et al. Engineering circular RNA for enhanced protein production. Nat Biotechnol 2023;41(2):262-72. (PMID: 35851375)

16. Geng Y, Wang M, Wu Z, Jia J, Yang T, Yu L. Research progress of circRNA in malignant tumour metabolic reprogramming. RNA Biol 2023;20(1):641-51. (PMID: 37599427)

17. Dong J, Zeng Z, Huang Y, Chen C, Cheng Z, Zhu Q. Challenges and opportunities for circRNA identification and delivery. Crit Rev Biochem Mol Biol 2023;58(1):19-35. (PMID: 36916323)

18. Wu J, Chen J, Hu J, et al. CircRNA Uxs1/miR-335-5p/PGF axis regulates choroidal neovascularization via the mTOR/p70 S6k pathway. Transl Res 2023;256:41-55. (PMID: 36690073)

19. Ju L, Yao M, Lu R, et al. Circular RNA hsa_circ_0051040 Promotes Hepatocellular Carcinoma Progression by Sponging miR-569 and Regulating ITGAV Expression. Cells 2022;11(22):3571. (PMID: 36429000)

20. Zheng J, Yan X, Lu T, et al. CircFOXK2 promotes hepatocellular carcinoma progression and leads to a poor clinical prognosis via regulating the Warburg effect. J Exp Clin Cancer Res 2023; 42(1):63. (PMID: 36922872)

21. Wang X, Dong F-L, Wang Y-Q, Wei H-L, Li T, Li J. Exosomal circTGFBR2 promotes hepatocellular carcinoma progression via enhancing ATG5 mediated protective autophagy. Cell Death Dis 2023;14(7):451. (PMID: 37474520)

22. Nishita-Hiresha V, Varsha R, Jayasuriya R, Ramkumar KM. The role of circRNA-miRNA-mRNA interaction network in endothelial dysfunction. Gene 2023;851:146950. (PMID: 36228866)

23. Liu J, Niu L, Hao J, Yao Y, Yan M, Li H. circIPO7 dissociates caprin-1 from ribosomes and inhibits gastric cancer cell proliferation by suppressing EGFR and mTOR. Oncogene 2023;42(13): 980-93. (PMID: 36732659)

24. Xu Q, Yao Y, Ni H, et al. Hsa-circ-0052001 promotes gastric cancer cell proliferation and invasion via the MAPK pathway. Cancer Med 2023;12(6):7246-57. (PMID: 36453441)

25. Dong J, Zheng Z, Zhou M, et al. EGCG-LYS Fibrils-Mediated CircMAP2K2 Silencing Decreases the Proliferation and Metastasis Ability of Gastric Cancer Cells in Vitro and in Vivo. Adv Sci (Weinh) 2023;10(32):e2304075. (PMID: 37752765)

26. Liu H, Fang D, Zhang C, et al. Circular MTHFD2L RNA-encoded CM-248aa inhibits gastric cancer progression by targeting the SET-PP2A interaction. Mol Ther 2023;31(6):1739-55. (PMID: 37101395)

27. Qiu F, Ou D, Tan H, Gao Y, Zi D. The circCDK17/miR-122-5p/ASF1B axis regulates the progression of cervical cancer. Histol Histopathol 2023;38(3):359-71, (PMID: 36178207)

28. Li Z, Cheng Y, Fu K, et al. Circ-PTPDC1 promotes the Progression of Gastric Cancer through Sponging Mir-139-3p by Regulating ELK1 and Functions as a Prognostic Biomarker. Int J Biol Sci 2021;17(15):4285-304. (PMID: 34803498)

29. Yu D, Zhang C. Circular RNA PTK2 Accelerates Cell Proliferation and Inhibits Cell Apoptosis in Gastric Carcinoma via miR-139-3p. Dig Dis Sci 2021;66(5):1499-509. (PMID: 32504353)

30. Zhang J, Hou L, Liang R, et al. CircDLST promotes the tumorigenesis and metastasis of gastric cancer by sponging miR-502-5p and activating the NRAS/MEK1/ERK1/2 signaling. Mol Cancer 2019;18(1):80. (PMID: 30953514)

31. Gao H, Xu J, Qiao F, Xue L. Depletion of hsa_circ_0000144 Suppresses Oxaliplatin Resistance of Gastric Cancer Cells by Regulating miR-502-5p/ADAM9 Axis. Onco Targets Ther 2021; 14:2773-87. (PMID: 33907420)

32. You W, Liu X, Yu Y, et al. miR-502-5p affects gastric cancer progression by targeting PD-L1. Cancer Cell Int 2020;20:395. (PMID: 32821248)

33. Liu M, Liu Q, Fan S, et al. LncRNA LTSCCAT promotes tongue squamous cell carcinoma metastasis via targeting the miR-103a-2-5p/SMYD3/TWIST1 axis. Cell Death Dis 2021;12(2):144. (PMID: 33542221)

34. Rong L, Chen B, Liu K, et al. CircZDBF2 up-regulates RNF145 by ceRNA model and recruits CEBPB to accelerate oral squamous cell carcinoma progression via NFκB signaling pathway. J Transl Med 2022;20(1):148. (PMID: 35365168)

35. Mi C, Zhang D, Li Y, et al. miR-4677-3p participates proliferation and metastases of gastric cancer cell via CEMIP-PI3K/AKT signaling pathway. Cell Cycle 2021;20(19):1978-87. (PMID: 34437815)